



Universidad Autónoma
de Madrid

Biblos-e Archivo
Repositorio Institucional UAM

Repositorio Institucional de la Universidad Autónoma de Madrid

<https://repositorio.uam.es>

Esta es la **versión de autor** del artículo publicado en:

This is an **author produced version** of a paper published in:

Journal of Catalysis 294 (2012): 207-215

DOI: <https://doi.org/10.1016/j.jcat.2012.07.023>

Copyright: © 2012 Elsevier Inc. This manuscript version is made available under the CC-BY-NC-ND 4.0 licence <http://creativecommons.org/licenses/by-nc-nd/4.0/>

El acceso a la versión del editor puede requerir la suscripción del recurso

Access to the published version may require subscription

Hydrodechlorination of dichloromethane with mono- and bimetallic Pd-Pt on sulfated and tungstated zirconia catalysts

J. Bedia^{a}, L.M. Gómez-Sainero^a, J.M. Grau^b, M. Busto^b, M. Martín-Martínez^a,
J.J. Rodríguez^a*

^a Sección de Ingeniería Química, Universidad Autónoma de Madrid, Cantoblanco, 28049 Madrid, Spain.

^b Instituto de Investigaciones en Catálisis y Petroquímica - INCAPE - (FIQ-UNL, CONICET), Santiago del Estero 2654, 3000 Santa Fe, Argentina.

**Telephone number: 34 91 4972911. Fax number: 34 91 4973516.*

E-mail: jorge.bedia@uam.es.

Abstract. Monometallic (Pt or Pd) and bimetallic (Pt-Pd) catalysts supported on zirconia promoted with sulfate (SZ) or tungsten oxide (WZ) were prepared and tested in the gas-phase hydrodechlorination of dichloromethane. The catalysts showed a high selectivity to non-chlorinated products (between 80 and 90 % at 250 °C) being methane the main reaction product. As a general trend, the WZ catalysts yielded significantly higher dichloromethane conversion than the SZ ones, reaching all the catalysts initial conversions higher than 80% at a reaction temperature of 250 °C. However, the former showed a very poor stability regardless of the metallic active phase. On the other hand, the presence of palladium in the sulfated zirconia catalyst avoids deactivation as proved in long-term experiments (80 h time on stream). XPS and elemental analyses of the used catalysts suggest that adsorption of organochlorinated species is a cause of deactivation by blocking the active sites. In the monometallic SZ Pt catalyst deactivation occurs also by poisoning of the Pt sites by the H₂S resulting from sulfate reduction under the hydrogen-rich gas atmosphere. The metal particle size appears to be a critical point to avoid the deactivation of the catalysts, those with higher dispersions show the highest stabilities with no signs of deactivation after more than 80 h of time on stream.

Keywords: *Sulfated zirconia, tungstated zirconia, hydrodechlorination, dichloromethane, palladium, platinum.*

1. Introduction

The emission of chlorinated volatile organic compounds (CVOCs) to the atmosphere contributes to ozone depletion, photochemical smog formation and global warming [1,2,3]. In particular, dichloromethane (DCM) is used as solvent in the chemical and pharmaceutical industries in the synthesis of different chemical compounds and polymers and for paint stripping and degreasing operations. Among the different removal techniques, catalytic hydrodechlorination (HDC) shows potential economic and environmental advantages when compared with other techniques.

In the last years, much effort has been focused in the study of the catalytic hydrodechlorination of CVOCs by catalysts based on different metals and supports. However, in the studies analyzing the gas-phase deep hydrodechlorination of chloroform and dichloromethane with supported metallic catalysts either a rapid deactivation has been reported or simply long-term experiments were not performed [4,5,6,7,8,9,10,11,12,13]. The stability of the hydrodechlorination catalysts is a key feature for industrial applications. Deactivation has been attributed to poisoning by HCl and chlorinated organic species, coke formation (in some cases including chlorine in its composition), loss of metal through the formation of volatile compounds and metal sintering, changes in the metallic oxidation state and metal migration [10,14,15,16,17,18,19,20]. The support plays a significant role in the activity and the stability of the catalysts [4,5,6,7,8,9,10,21], its surface acidity seems to play a key role in deactivation.

Our research group has previously investigated the gas-phase hydrodechlorination of dichloromethane and chloroform using Pd on activated carbon (Pd/C) catalysts, which showed high activity and high selectivity to non-chlorinated products [22,23,24,25,26]. However these catalysts underwent significant deactivation due to the irreversible

chemisorption of reactants and/or reaction products on the active sites. A comparative study [23] on the behavior of Pd, Ru, Pt, and Rh catalysts supported on activated carbon in the hydrodechlorination of DCM showed that Pd/C and Rh/C were the most active catalysts but Pt/C showed the highest stability with no sign of deactivation after 65 h on stream. More recently [27], a Pt/C catalyst prepared in our lab showed a very high stability with no significant loss of activity after 26 days on stream, which had not been previously reported. It seems that a high Pt^0/Pt^{n+} ratio favors the stability of the catalyst since Pt^0 appears to be more resistant than Pt^{n+} to poisoning by organochlorinated compounds. The Pt^0/Pt^{n+} ratio could be controlled with the reduction temperature. Higher reduction temperatures assure a higher proportion of zerovalent platinum, although if the reduction temperature is excessively high an agglomeration of the catalysts particles could happen with the consequent decrease in the dispersion values. Based on preliminary studies [28] we have selected a proper reduction temperature in order to obtain catalysts with a high Pt^0/Pt^{n+} ratio and with low catalysts particle sizes. On the other hand, re-dispersion of metal particles was observed in the Pt/C catalyst [27] leading to non agglomerated small particles well distributed on the support, which contribute to increase the concentration of H_2 in the vicinity of the active sites and its spillover in the catalytic surface. This appears to favor the reaction of H_2 with the adsorbed chlorinated hydrocarbons, thus inhibiting the poisoning of the catalyst [27]. Therefore, the high resistance of Pt/C to poisoning by these compounds when compared to other catalysts reported in the literature can be attributed to redispersion of Pt during the reaction which leads to much smaller metal particles which are very homogeneous in size, show very little agglomeration and are well distributed over the support. It is proposed that these factors would inhibit the formation and stabilization of higher hydrocarbons than CH_4 at the active centers.

In order to confirm the role of the metallic particle size and distribution over the support in the stability of the catalysts in the HDC of chloromethanes, in this work, the performance of catalysts prepared from supports with a very different nature than that of carbon, but allowing to obtaining a wide range of dispersions of the active phase, is investigated. This may contribute to a rational design of future catalysts providing a real benefit to catalyst technology.

Taking into account the key role of the acidity of the support in the dispersion of the metallic phase and the deactivation of the catalysts, it is of interest to investigate the development of catalysts with a good balance between the metallic and acidic functions. The objective of this work is to analyze the activity, selectivity and stability of different mono- and bimetallic Pd-Pt catalysts based on acidic supports, like sulfated (SZ) and tungstated (WZ) zirconia, in the hydrodechlorination of dichloromethane. The selection of metals was made by considering the great stability of Pt and the high activity of Pd [23,27]. Moreover, the use of bimetallic catalysts often results in an increase of the metallic dispersion. In fact, the novel catalytic system SZ Pt-Pd found in this study shows the same stability and selectivity that our previous Pt/C catalysts [27] but with a significant increase in the activity.

2. Experimental

2.1. Catalyst preparation

Monometallic (Pd or Pt) and bimetallic (Pd and Pt) catalysts were supported on sulfated and tungstated-promoted zirconia. The SO_4^{2-} -ZrO₂ support (SZ) was obtained from commercial material in the form of a powdered sulfate-doped hydroxide gel (SZOH) (Grade XZO 1249/01, 7.6 wt.% S on ZrO₂ basis) and the WO₃-ZrO₂ support (WZ) was

obtained from commercial material in the form of a powdered tungstated-doped hydroxide gel (WZOH) (Grade XZO 1251/01, 16 wt.% W on ZrO_2 basis). Both commercial materials were supplied by MEL Chemicals. These supports were first pressed and shaped into cylindrical pellets using a hydraulic press (8 Ton cm^{-2}). Then the pellets were ground and sieved to 35–80 meshes. Samples were taken and subjected to calcination in a muffle furnace in static air for 3h at 600°C in the case of SZOH and at 800°C in the case of WZOH, temperatures that were confirmed in previous studies as optimal for obtaining a crystalline tetragonal zirconia with a proper amount of acidic sites [29,30]. In each calcination treatment the catalyst was first heated from room temperature to 180°C at $2^\circ\text{C}\cdot\text{min}^{-1}$ in air and this temperature was held for 1 h. Then the temperature was increased at a heating rate of $5^\circ\text{C}\cdot\text{min}^{-1}$ up to 600°C or 800°C and held for another 3 h. The sample was then cooled down to room temperature.

The resulting crystalline solids (SZ and WZ, for sulfated and tungstated zirconia supports, respectively) were then impregnated at room temperature with chloroplatinic acid ($\text{H}_2\text{Cl}_6\text{Pt}\cdot 6\text{H}_2\text{O}$, Sigma-Aldrich, $\leq 99.9\%$, CAS Number: 26023-84-7) and/or palladium chloride (Cl_2Pd , Sigma-Aldrich, $\leq 99.9\%$, CAS Number: 7647-10-1) aqueous solutions by the incipient wetness method. The amount of solution was regulated to obtain nominal 0.5% Pt or Pd in the final catalyst. Once impregnated the samples were maintained 24 h at room temperature and then dried slowly in a stove. The temperature was raised slowly from ambient to 110°C in order to prevent the solvent carrying over the metal precursor to the pore mouths. The samples obtained were denoted as SZ-Pd and SZ-Pt for the palladium and platinum sulfated zirconia, respectively, and WZ-Pd and WZ-Pt for the palladium and platinum tungstated zirconia, respectively. In the case of the bimetallic catalysts, the supports (SZ and WZ) were impregnated first with a chloroplatinic acid solution by the incipient wetness method.

Then the impregnated samples were maintained 24 h at room temperature, subsequently dried at 120 °C and finally calcined in air for 1 h at 500 °C to assure the removal of water and the decomposition of the metallic precursor. Afterwards incipient wetness impregnation was accomplished with palladium chloride solution. Once again, the impregnated samples were maintained 24 h at room temperature, subsequently dried at 120 °C and finally calcined in air for 1 h at 500 °C to assure the removal of water and the decomposition of palladium chloride. The concentrations of Pt and Pd in the impregnation solution were adjusted in order to get a nominal 0.325% Pt and 0.175% Pd in the final catalyst. These weight percentages yield a Pt:Pd atomic ratio of 1:1. The samples obtained were named SZ Pd-Pt and WZ Pd-Pt, for the bimetallic catalysts supported on sulfated and tungstated zirconia, respectively.

2.2. Catalyst characterization

The pore structure of the catalysts fresh and once used in the HDC reaction was characterized from 77 K N₂ adsorption–desorption using a Micromeritics TriStar apparatus. The samples were previously outgassed for at least 8 h at 150 °C at a residual pressure of 10⁻³ Torr. From the N₂ adsorption-desorption isotherms, the apparent surface area (A_{BET}) was determined applying the BET equation [31], the total pore volume was calculated from the amount of nitrogen adsorbed (as liquid) up to a relative pressure of 0.95.

The X-ray diffraction (XRD) patterns of the catalysts and supports were obtained in a X'Pert PRO Panalytical Diffractometer. The powdered sample was scanned using Cu K α monochromatic radiation ($\lambda = 0.15406$ nm) and a Ge mono filter. A scanning range of $2\theta = 20\text{--}75^\circ$ and scan step size of 0.020° with 5 s collection time were used.

The elemental analyses of the samples were performed in a Leco CHNS-932 system. Inductive coupled plasma-mass spectroscopy (ICP-MS) was used to analyze the bulk Pd and Pt content, by means of a model Elan 6000 Sciex Perkin Elmer apparatus. (Metemos lo de Javier en vez de esto?) The surface of the catalysts was analyzed by X-ray photoelectron spectroscopy (XPS) with a Physical Electronics 5700C Multitechnique System, using Mg K α radiation ($h\nu = 1253.6$ eV). To determine all the elements present on the catalyst surface, general spectra were recorded for the samples by scanning the binding energy (BE) from 0 to 1200 eV. Binding energy values were corrected for the effects of sample charging by taking the C 1s peak (284.6 eV) as an internal standard. The accuracy of the BE scale was ± 0.1 eV. The deconvolution procedure involved smoothing, a Shirley background subtraction, and curve fitting using mixed Gaussian–Lorentzian functions by a leastsquares method. The atomic ratios of the elements were calculated from the relative peak areas of the respective core level lines using Wagner sensitivity factors [32].

Micromeritics ChemiSorb 2705 pulse analyzer was used to measure the catalysts dispersion by CO chemisorption at room temperature. Several pulses of 50 μ L CO were then introduced until saturation of the catalyst surface was achieved. The number of exposed metallic atoms was calculated from CO chemisorption data. The stoichiometry of the adsorption of CO over the metallic atoms was assumed to be 1 [33,34].

XRD, XPS, CO chemisorption and 77 K N₂ adsorption–desorption were performed with the catalysts calcined at 450 °C under air flow, subsequently reduced at 300 °C for 2 h under hydrogen flow and then cooled down to room temperature under helium flow. The reducibility of the metallic phase of the catalysts was analyzed by temperature programmed reduction (TPR) in an Ohkura TP2002 apparatus equipped with a thermal conductivity detector. The samples (0.15 g) were first activated by calcination in air at

450 °C. Then they were stabilized in Ar at 100 °C, cooled to room temperature and finally heated to 800 °C at a 10 °C·min⁻¹ rate in a stream of 4.8% H₂ in Ar.

2.3. Catalytic activity experiments

The activity of the catalysts in the hydrodechlorination of dichloromethane was evaluated in a continuous flow reaction system described elsewhere [22], consisting basically of a 4.0 mm i.d. quartz fixed bed micro-reactor (Microactivity Reference, PID Eng&Tech, Spain) coupled to a gas chromatograph (Varian, model 450GC) equipped with a FID detector and a capillary column (Varian, CP-SilicaPLOT, 60 m) for the analysis of the reaction products. The catalysts were treated “in situ” by calcination in air at 450 °C (50 Ncm³ min⁻¹) and reduction in hydrogen stream (50 Ncm³ min⁻¹) for 1 h at 300 °C prior to reaction. The experiments were performed at atmospheric pressure using an inlet total flow rate of 100 Ncm³ min⁻¹ and a H₂/DCM molar ratio of 100 at a space time of 0.8 kg_{cat}·h·(mol DCM)⁻¹. The gas feed contained a DCM concentration of 1000 ppmv and was prepared by mixing appropriate proportions of a commercial mixture of dichloromethane and N₂ (4000 ppmv of DCM in N₂) with pure N₂. Reaction temperatures within the range of 150–250° C were tested. For the sake of checking possible mass-transfer limitations, a previous series of experiments was performed at 250° C varying the total flow rate and the catalyst particle size. No significant changes were found in DCM conversion for gas velocity and particle size within the ranges of 0.02–0.06 m/s and 0.25–0.71 mm, respectively. The behavior of the catalysts was analyzed in terms of DCM conversion (X) and selectivities to the different reaction products (S_i). The evolution of the catalytic activity upon time on stream was also studied. The carbon mass balances were checked and they matched always within 91–99%. The experimental results were reproducible with less than 5% error.

3. Results and discussion

3.1. Catalyst characterization

Table 1 reports the BET surface area and total pore volume of the catalysts prepared. The N₂ adsorption-desorption isotherms correspond to type IV of IUPAC classification characteristic of mesoporous solids with low contribution of microporosity as indicated by the low amount of nitrogen adsorbed at low relative pressures. The catalysts based on SZ support show a more developed porosity than the WZ-based as indicate the higher values of surface area and pore volume, probably a consequence of the lower activation temperature (600 °C) of the SZOH hydroxide gel compared to that of the WZOH hydroxide gel (800 °C). No significant differences can be observed between the catalysts prepared with the same support.

Table 1. Porous structure of the catalysts.

Catalyst	A _{BET} (m ² /g)	Pore volume (cm ³ /g)
SZ Pt	116	0.176
SZ Pd	113	0.173
SZ Pt-Pd	112	0.175
WZ Pt	47	0.119
WZ Pd	48	0.122
WZ Pt-Pd	49	0.121

Figure 1 shows the TPR profiles of the catalysts. The SZ series shows only the peaks associated with the reduction of the metallic species. That of SZ Pt displays a peak associated to the reduction of the platinum species at 166 °C and the TPR profile of SZ Pd shows a peak centered at 102 °C with a shoulder 116 °C, related to the reduction of palladium. This indicates a stronger interaction of platinum with the support. In the case of the bimetallic SZ Pt-Pd catalyst, it appears only one peak, centered at around 116 °C. Besides, the absence of peak at 166 °C in the TRP profile of SZ Pt-Pd catalyst indicates

that there exists some kind of interaction between both metals. This type of interaction between Pd and Pt has been previously reported in bimetallic silica-alumina-supported catalysts [35,36]. It is possible that the metal precursor reduced first, which according to the TPR profiles of the monometallic samples should be palladium, can supply dissociated hydrogen that contributes to the reduction of the second metal (platinum). In contrast with WZ Pd, in the case of the SZ Pd catalysts there is no evidence for Pd hydride decomposition as the negative peak is not advised. It is probably a consequence of the different type of interaction of Pd and the two different supports SZ and WZ. The TPR profiles of WZ catalysts show several peaks of metal reduction which denotes a higher heterogeneity in the location of metal particles onto the support. In contrast with the SZ series, the catalysts containing Pd show a reduction peak at higher temperature than that of Pt (maxima at 168 °C and 145 °C, respectively). On the other hand, these WZ catalysts, specially the WZ Pd, show a negative peak at temperatures between 111 °C and 129 °C which can be attributed to hydrogen desorption from decomposition of mobile palladium hydrides previously formed at low temperature [37,38], indicative of the reduction of metallic particles at low temperature. In the case of the SZ Pd catalysts there is no evidence for Pd hydride decomposition probably as a consequence of the different type of interaction of Pd and the two different supports SZ and WZ. The peaks displayed above 300 °C correspond to the reduction of tungsten oxide species [39].

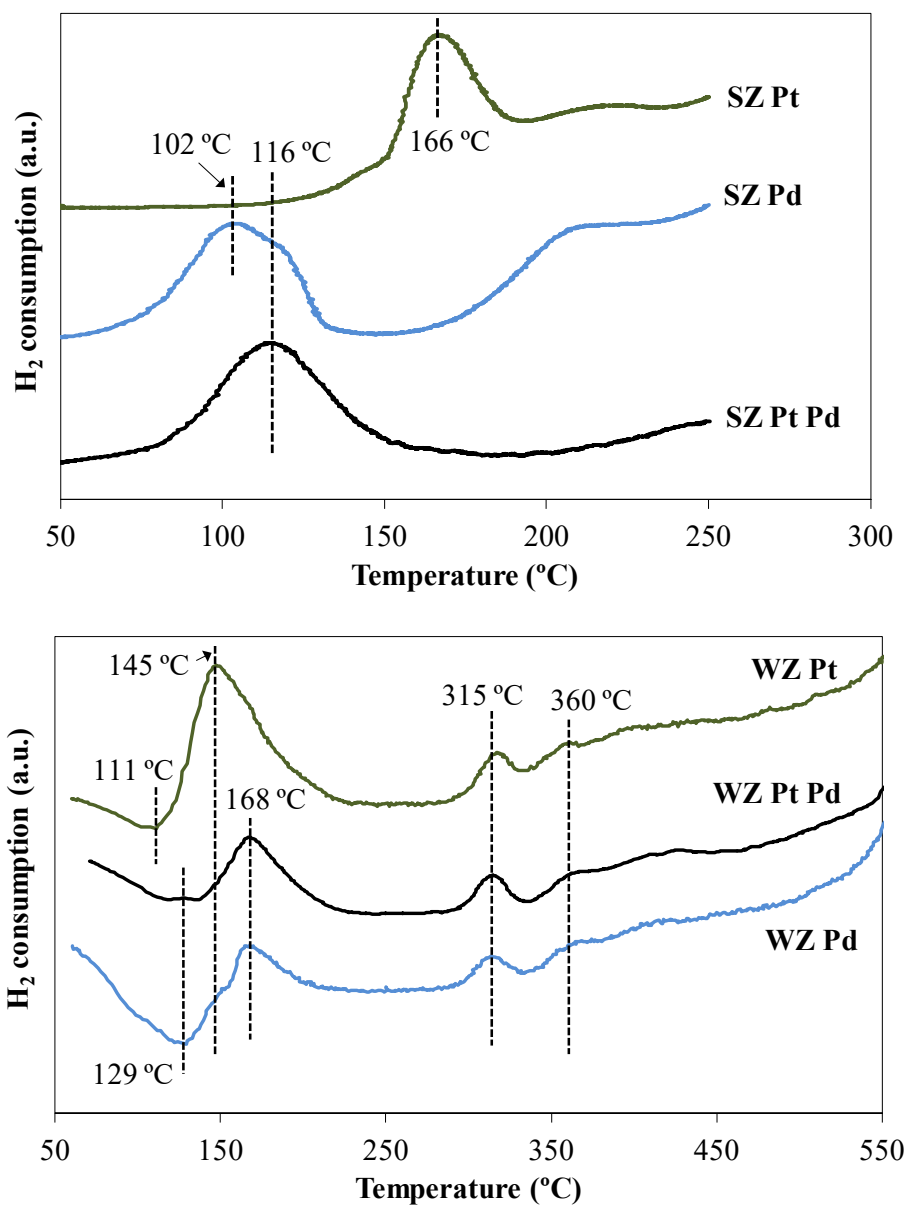


Figure 1. TPR profiles of the catalysts.

The chemical analysis (ICP) confirmed that the percentage of Pt and Pd was not modified by the calcination and/or reduction treatments and that the real content lied within $\pm 7\%$ of the theoretical value calculated from the amount of precursor impregnated. Table 2 summarizes the elemental mass surface concentrations of Pt and Pd obtained by XPS. As can be seen, the mass surface concentration of platinum in the monometallic catalysts (0.6%) is only somewhat higher than the bulk one (0.5%) while

important differences are observed for the bimetallic and SZ Pd catalysts, more noticeable for the SZ Pt-Pd which yielded mass surface concentrations of palladium and platinum significantly higher than the corresponding bulk contents. This indicates that the metal particles must be predominately located in the most external surface of the catalyst (since XPS allows to determine only the chemical composition of the outermost layer) approaching to an egg-shell type distribution. It is also worth mentioning that despite the use of chlorine-containing precursors (chloroplatinic acid and palladium chloride) no surface chlorine was detected in the XPS analyses of the SZ samples in contrast with the around 0.5 wt% detected for the WZ catalysts.

Table 2. Surface concentration (by XPS) of Pt and Pd (w%) and metal dispersion (%) of the catalysts prepared.

Catalyst	%Pd	%Pt	D (%)
SZ Pt	--	0.6	19
SZ Pt-Pd	1.0	0.7	28
SZ Pd	0.8	--	16
WZ Pt	--	0.6	14
WZ Pt-Pd	0.6	0.3	12
WZ Pd	0.7	--	16

The Pt 4f region of the XPS spectra for all the catalysts showed a doublet corresponding to Pt 4f_{5/2} and Pt 4f_{7/2} [40]. The separation between Pt 4f_{5/2} and Pt 4f_{7/2} peaks, due to spin orbital splitting, is a quantized value of 3.33 eV. The Pt 4f_{7/2} peak lying at around 71.0 eV can be attributed to Pt⁰ (zerovalent Pt), while the Pt 4f_{7/2} peak located at around 72.3 is related to Ptⁿ⁺ (electrodeficient Pt). Figure 2 represents the deconvoluted Pt 4f spectra of the SZ Pt-Pd catalyst. Pt in this catalyst is present mainly as Pt⁰, with a lower fraction of Ptⁿ⁺. The values of the atomic ratio of surface platinum species (Pt⁰ and Ptⁿ⁺) for the different platinum-containing catalysts, as obtained by deconvolution of the XPS Pt 4f region, are summarized in Table 3. As can be seen, Pt⁰ is by far the predominant

state in all the cases as a result of the reduction step. It would be also interesting to deconvolute the Pd 3d spectra. However, in the case of the catalysts containing Zr and Pd, the Pd 3d_{5/2} and Zr 3p_{3/2} XPS spectra are overlapped. Some authors [41,42], which used Pd (1%wt) supported on zirconia catalysts, subtract the contribution of the Zr 3p signal from the total spectra and associate the rest of the spectra to the Pd 3d response which could be deconvoluted. However, in this study, with fairly low palladium contents (0.5%wt for monometallic and 0.175%wt for bimetallic catalysts), this method does not allow obtaining reliable results of the relative amounts of zerovalent and electrodeficient palladium.

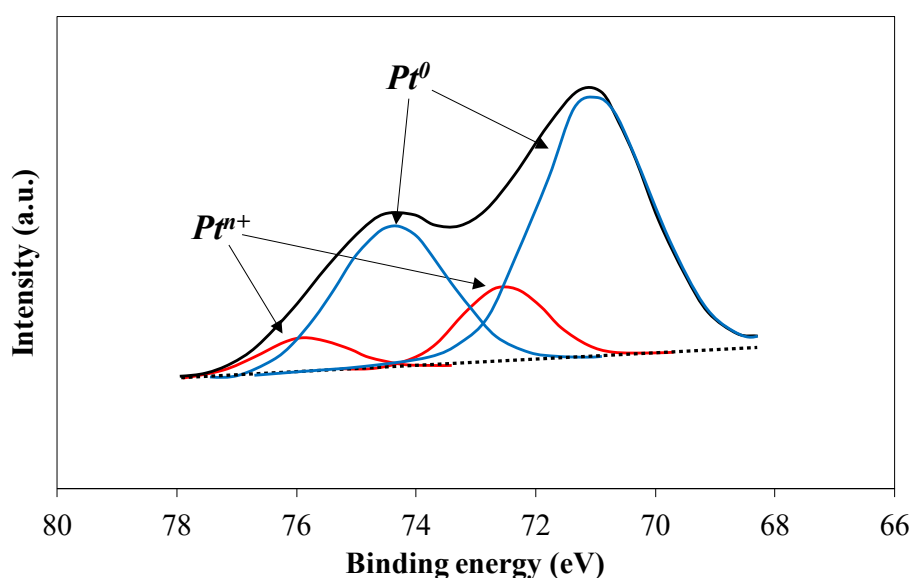


Figure 2. Deconvoluted Pt 4f spectra of the SZ Pt-Pd catalyst.

Table 3. Pt⁰/Ptⁿ⁺ atomic ratio on the surface of the catalysts.

	Pt ⁰ /Pt ⁿ⁺
SZ Pt	3.0
SZ Pt-Pd	4.8
WZ Pt	7.9
WZ Pt-Pd	4.3

The XRD patterns of the catalysts are represented in Figure 3. All the diffractograms showed the main peaks of monoclinic (m-ZrO₂) and tetragonal (t-ZrO₂) phases of zirconia [43]. In the case of the WZ catalysts, the main peaks associated to WO₃ phase are observed. The peaks associated to oxides of platinum and palladium were not seen in any of the diffractograms, whether due to the absence of metal oxide particles in these samples or because those particle are too small or non crystalline. According to the XPS results a small amount of metal oxide particles could be expected (Table 3). The peaks associated to zerovalent platinum and zerovalent palladium are located at 2θ values of 39.8° and 40.1°, respectively [44]. Figure 4 shows more in detail the XRD spectra of the catalysts within the 2θ range of 39-41°. The peaks corresponding to zerovalent platinum or zerovalent palladium were not observed in the spectra of SZ catalysts. This suggests that the metal particles are of small size and relatively well dispersed so therefore they do not produce XRD reflections. However, Figure 4 shows clearly peaks at 2θ = 39.8° related with Pt⁰ in the WZ Pt and WZ Pt-Pd catalysts. This indicates that these catalysts contain larger platinum particles and suggests a poorer metal dispersion. The lower acidity of WZ compared to SZ [45] support may explain that poorer dispersion since it is well known that acidic groups increase the hydrophilic character of the support, thus favoring the diffusion of the metal precursor [46,47,48].

These results are in agreement with the metal dispersions obtained by CO chemisorptions reported in Table 2 where the lowest dispersion values are associated with the WZ Pt and WZ Pt-Pd catalysts, the ones with the highest metal particle sizes as suggested by the XRD diffractograms. Furthermore, the catalyst with the highest metal dispersion and consequently the lower metal particle size is the SZ Pt-Pd. Although, CO chemisorption cannot distinguish between Pd and Pt and possible bimetallic formation

can complicate matters further in terms of CO uptake, the significant higher dispersion value indicates suggest lower particle sizes well in monometallic or in bimetallic form.

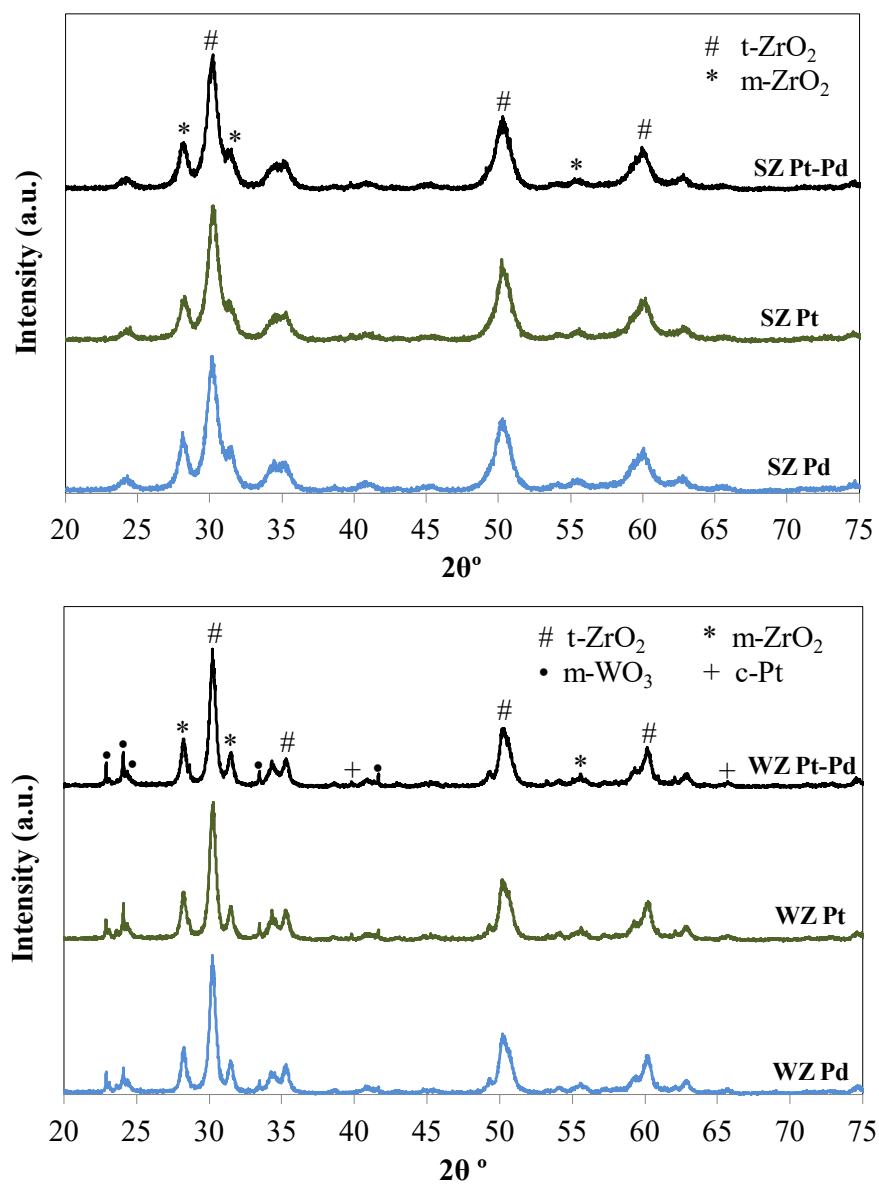


Figure 3. XRD patterns of the catalysts.

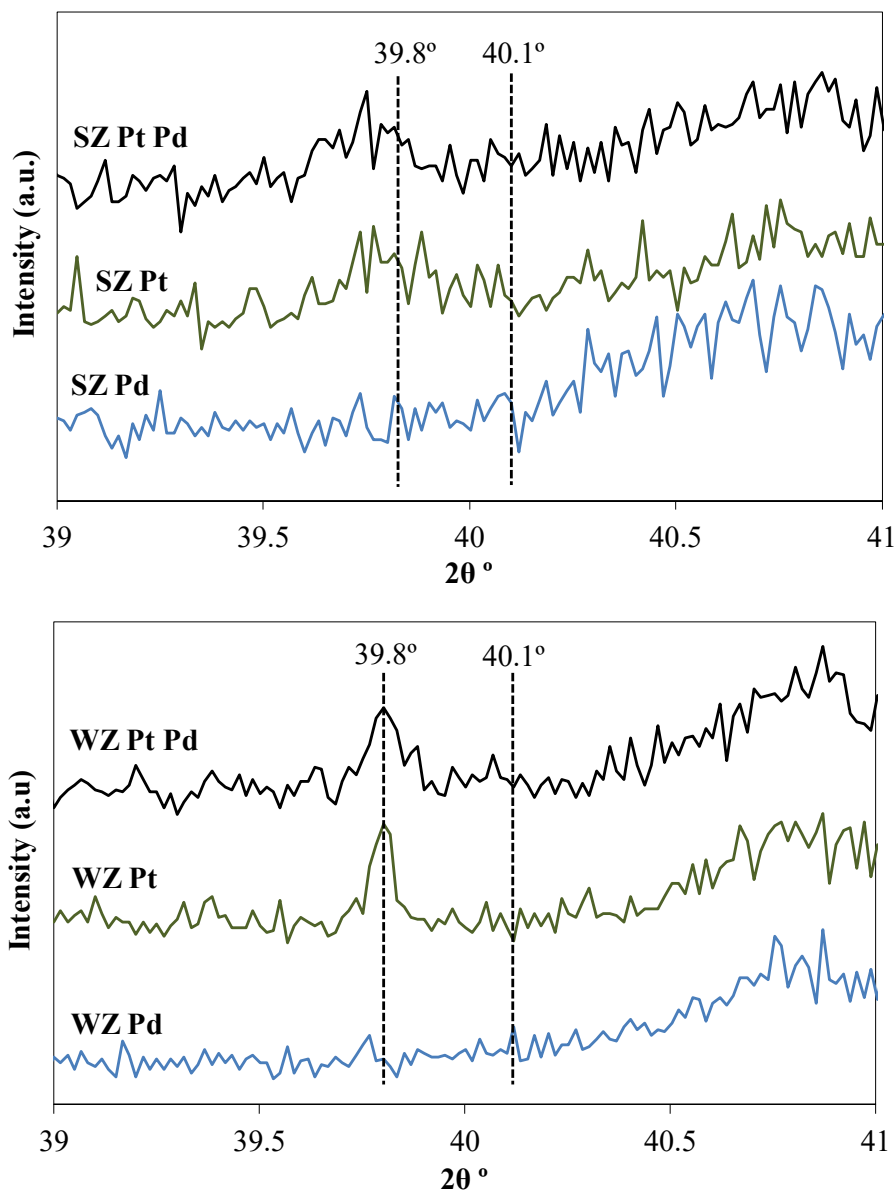


Figure 4. Detail of the XRD patterns of Figure 3.

3.2. Catalytic activity

The absence of mass transfer limitations at the reaction conditions was verified theoretically. The external diffusion mass transfer resistance was evaluated by the estimation of the Damköhler number [49]. The influence of internal mass transfer was evaluated using the criterion of Weisz [50], according to which internal mass transfer effects can be neglected for values of the dimensionless Weisz number lower than 0.15

[50]. In the most unfavorable conditions, the values of the Damköhler and Weisz number fall well below 0.1 and 0.15, respectively, within the temperature range used in this work, thus allowing to neglect mass-transfer limitations in our experimental conditions according to the Carberry criteria [49]. Taking into account the diluted DCM concentration it can be assumed that thermal effects are negligible.

Figure 5 shows the values of DCM conversion obtained at a space time of $0.8 \text{ kg}_{\text{cat}} \cdot \text{h} \cdot (\text{mol DCM})^{-1}$ and different reaction temperatures with the SZ and WZ catalysts. A dramatic increase of conversion with temperature was observed within the range explored (150-250 °C). As can be seen, with the exception of the monometallic Pt catalysts, the WZ series yielded significantly higher DCM conversion than the SZ, although the differences become lower as the temperature increases. The bimetallic WZ Pt-Pd catalyst allowed almost complete DCM conversion. Whereas the three catalysts of the SZ series show a fairly similar behavior, in the WZ series the Pd-containing catalysts were significantly more active than the monometallic Pt one. This second trend is in agreement with the observed in a previous work [23] where activated carbon-supported Pd and Pt catalysts were compared.

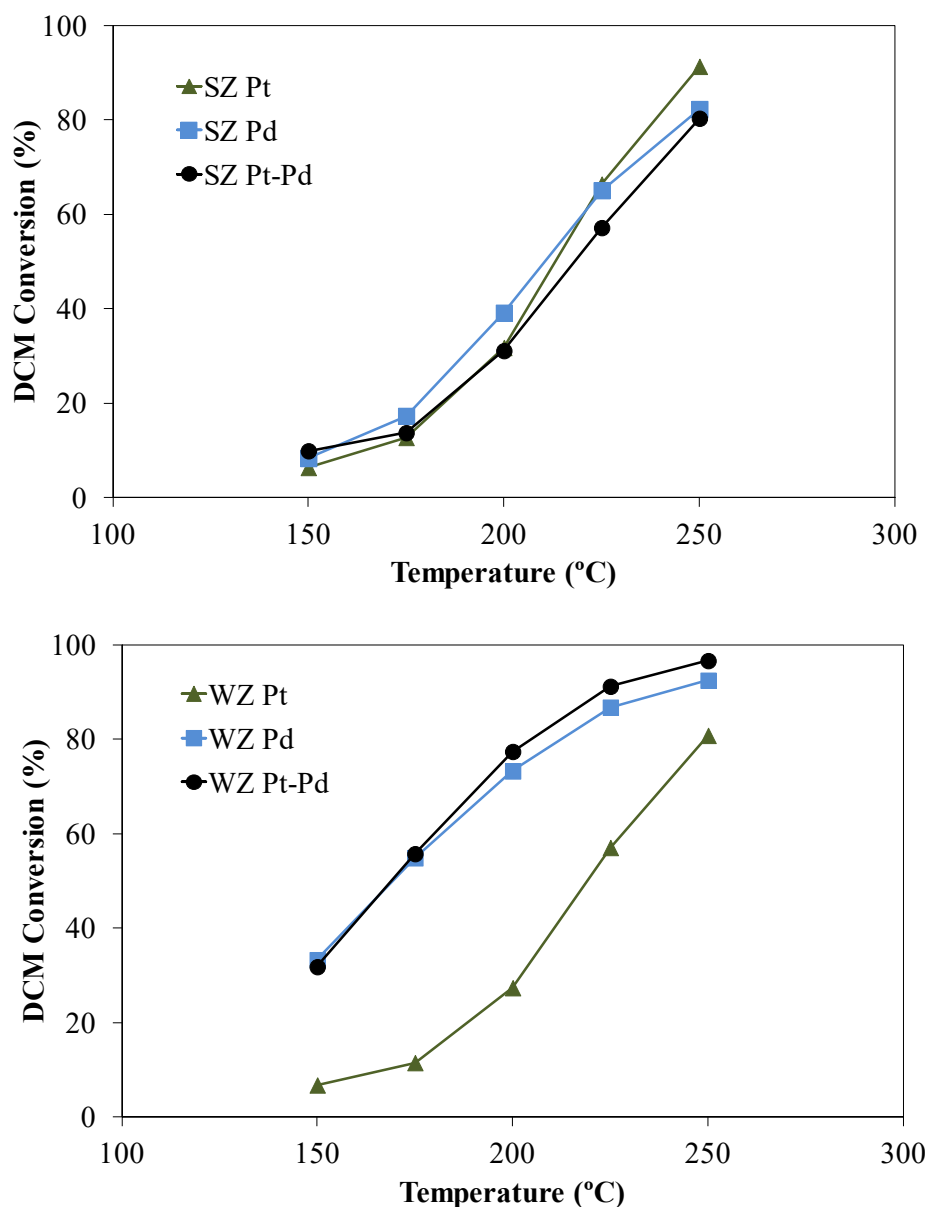


Figure 5. DCM conversion upon HDC at a space time of $0.8 \text{ kg}_{\text{cat}} \cdot \text{h} \cdot (\text{mol DCM})^{-1}$ and different reaction temperatures with the SZ and WZ catalysts.

Figure 6 shows the selectivity to reaction products of the monometallic Pd catalysts at a space time of $0.8 \text{ kg}_{\text{cat}} \cdot \text{h} \cdot (\text{mol DCM})^{-1}$ and different reaction temperatures. As depicted in Figure 5 both Pd catalysts yielded high DCM conversions at the highest temperature tested (250 °C) although the WZ-supported was significantly more active (93% DCM conversion versus 82% of the SZ-supported). The selectivity curves

obtained for the rest of the catalysts are reported as Supplementary information. Hydrodechlorination of DCM with all the catalysts tested yielded the following non-chlorinated reaction products: methane, ethane, propane, n-butane and 1-butene. In addition, propylene and ethylene were detected but only in the long-term experiments performed for analyzing the stability of the catalysts. All the catalysts were very selective to non-chlorinated byproducts and the selectivity to monochloromethane (MCM) decreased when increasing the temperature with the exception of the monometallic Pt catalysts (SZ Pt and WZ Pt) where that selectivity remained almost constant within the temperature ranged tested (see Supplementary information). At the highest temperature tested (250 °C) the selectivity to non-chlorinated byproducts ranged between 80 and 90%. The main reaction product was always methane with selectivities from around 60% up to more than 85% (for SZ Pt-Pd at 250 °C). As a general conclusion, the selectivity to methane was lower with the WZ-supported catalysts, especially with the WZ Pd catalyst. In previous works [27,51], dealing with the HDC of DCM, higher selectivities to methane were observed with well dispersed Pd/C and Pt/C catalysts with higher proportions of metal in the zero-valent state. The formation of hydrocarbons higher than CH₄ has been previously related with the electro-deficient metal species, and the presence of large agglomerated metal particles [22,25,27,52]. This is in agreement with our results, where those large particles were observed by XRD in the WZ-supported catalysts (Figure 4). Previous works on the hydrodechlorination of DCM and carbon tetrachloride with carbon-supported Pd catalysts [22,25,52] showed the existence of dual active sites formed by the connection of adjacent zero-valent and electroneficient palladium species (Pd⁰ + Pdⁿ⁺). In these cases, hydrogen chemisorbs and homolytically dissociates on Pd⁰, while the chloromethane molecule is chemisorbed on Pdⁿ⁺. Therefore, the formation of

hydrocarbons of more than one C atom seems to be associated with the reaction of two organochloride radicals adsorbed on neighboring electro-deficient metal sites. Thus, a lower concentration of these sites on the catalyst would reduce the formation of those byproducts and, according to previous works [52], when they are formed, the temperature has a significant effect on the products distribution, the selectivity to those species being favored in detriment of methane by increasing the temperature. In our case, slightly higher selectivities to hydrocarbons higher than methane (C_2H_6 , C_3H_8 and $i-C_4H_{10}$) were observed with the WZ-supported catalysts as well as an increase of the selectivity to these compounds with the reaction temperature, which could be consequence of higher amounts of electrode deficient species in these catalysts.

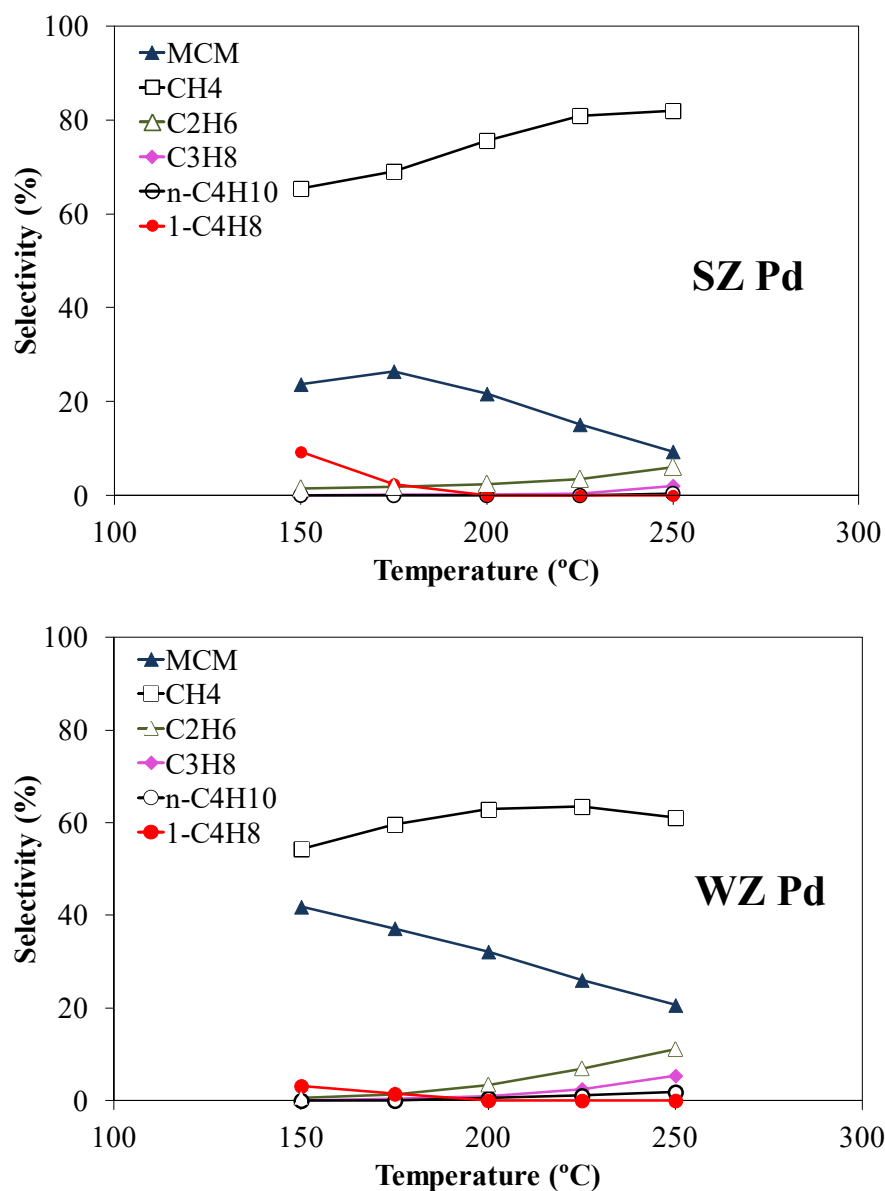


Figure 6. Selectivity of monometallic Pd catalysts at a space time of $0.8 \text{ kg}_{\text{cat}} \cdot \text{h} \cdot (\text{mol DCM})^{-1}$ and different reaction temperatures.

Table 4 compares the reaction temperature and the selectivity of the main products, namely CH₄ and MCM, at a fixed DCM conversion of 50%. As can be seen in this table, in general trend, the catalysts of the SZ series, result in higher selectivities to non-chlorinated byproducts. This support appears to favor the supply of H₂ to the active centers as lower selectivities to MCM are obtained at all reaction temperatures (see data

for SZ Pd and WZ Pd in Figure 6). Nevertheless, the high MCM selectivity values obtained for WZ Pd and WZPt-Pd at 50% of conversion can be attributed to the lower reaction temperature which has a marked influence in the selectivity to this product (Figure 6). The comparison of the selectivities to the different reaction products with the reaction temperature suggest that the increase of the temperature results in higher selectivities to non-chlorinated byproducts.

Table 4. Reaction temperatures and selectivity to the main products at a fixed DCM conversion of 50%.

	T (°C)	S _{CH₄} (%)	S _{MCM} (%)
SZ Pt	214	72.7	24.7
SZ Pt-Pd	220	79.6	19.3
SZ Pd	209	78.1	18.2
WZ Pt	224	71.7	23.5
WZ Pt-Pd	172	67.1	30.3
WZ Pd	173	58.2	38.3

3.3. Catalysts stability

In the literature, the deactivation of the catalysts in HDC is attributed to poisoning by HCl and other chlorine compounds, deposition of coke or organochloride species, metal sintering, loss of metal by the formation of volatile compounds and changes in the oxidation state of the metal [4,15,16,17,18,19,20,53,54]. In general, the catalysts show an initial unsteady state with a significant decrease of the activity before a steady residual activity is reached. The development of highly stable catalysts for hydrodechlorination and the analysis of the causes of deactivation has received increasing attention [27,55,56,57,58,59,60,61,62].

Figure 7 shows the evolution of DCM conversion upon time on stream (tos) in long-term experiments performed at a space time of $0.8 \text{ kg}_{\text{cat}} \cdot \text{h} \cdot (\text{mol DCM})^{-1}$ and 250 °C with the SZ and the WZ catalysts. All the catalysts supported on tungstated zirconia (WZ series) showed a very poor stability regardless of the metal active phase. On the

contrary, the SZ-supported catalysts containing Pd exhibited a highly stable behavior, especially in the case of the bimetallic catalyst. It can be seen that the SZ Pd catalyst suffers a slow but monotonical loss of activity upon the 80 h on stream of the experiment whereas the SZ Pt-Pd showed no deactivation and even a sustained increase of DCM conversion with time on stream was observed. The TPR profiles of these two catalysts (Figure 1) suggest a fairly uniform distribution of the metallic particles, more remarkable in the case of the bimetallic catalyst, whose XRD spectrum (Figure 2) and CO chemisorptions metal dispersion value (Table 2) suggest also a good dispersion of the metallic particles which are predominantly located on the outer surface of the support as suggested by XPS results of Table 2. These features must favor the adsorption, desorption and spillover of reactants and/or reaction products which in turn enhances the deep hydrogenation of chlorocarbons and hinders their irreversible adsorption on the active sites. Figure 7 shows an apparent initial decline in conversion with time on stream for SZ Pt-Pd and SZ Pd suggesting some surface restructuring. Several authors ascribe some surface restructuring of metallic particles to the effect of HCl which they report to provoke the formation, volatilization, and re-deposition of unstable metallic chlorides [15,63]. These chlorides would be reduced in the high concentration of H₂ introduced as a reactant

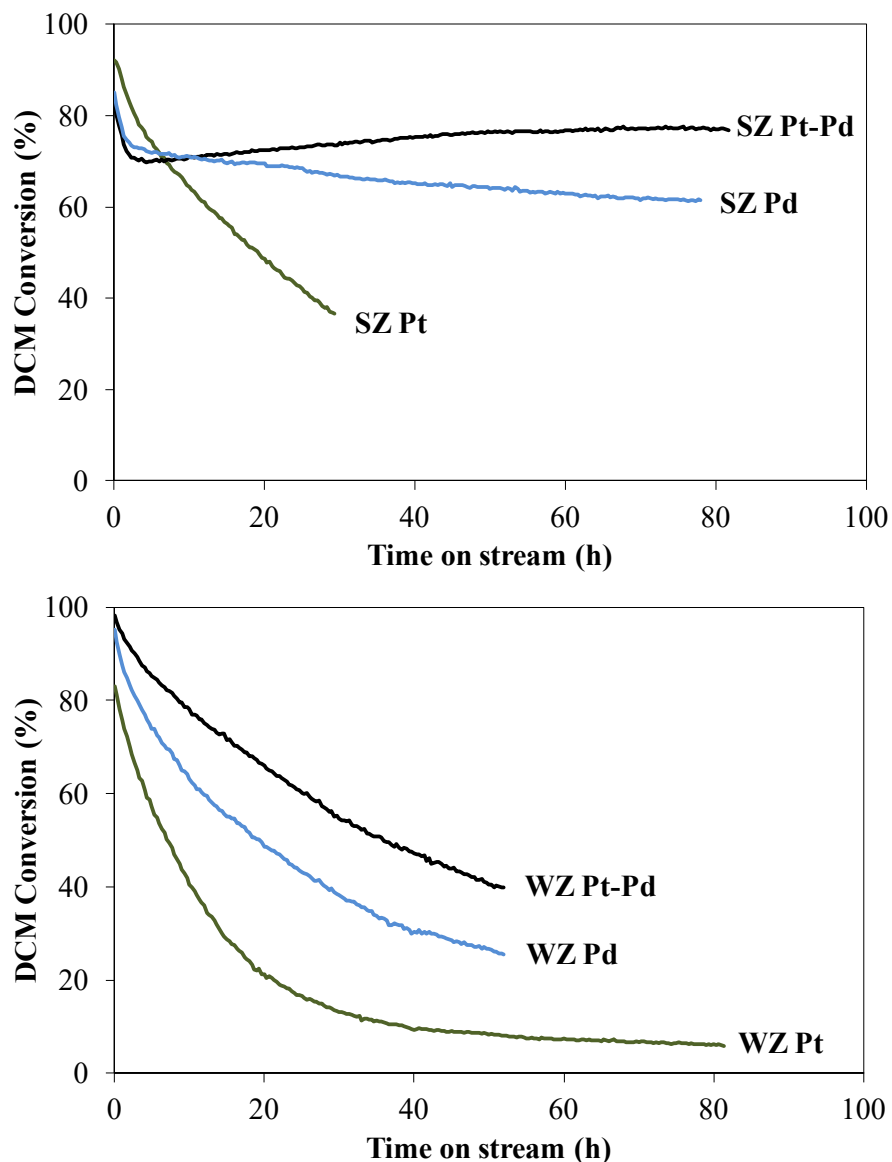


Figure 7. Evolution of DCM conversion upon time on stream in long-term experiments with the catalysts tested (space time = $0.8 \text{ kg}_{\text{cat}} \cdot \text{h} \cdot (\text{mol DCM})^{-1}$; $T = 250 \text{ }^{\circ}\text{C}$).

Figure 8 depicts the selectivity to reaction products upon time on stream from the experiment of Figure 7 for the highly stable SZ Pt-Pd catalyst. After the initial transition period no significant changes in the selectivities to the different reaction products were observed. As stated before, methane was the main reaction product with a selectivity around 80% and the selectivities to the chlorinated byproduct, MCM, remained relatively low at around 15%. The rest of the reaction products (total selectivity lower

than 5%) were mainly ethane with lower amounts of propane and traces of n-butane and 1-butene. A similar behavior was observed for SZ Pd catalyst (see Figure S5 of Supplementary information), the other one showing a fairly stable behavior (Figure 7).

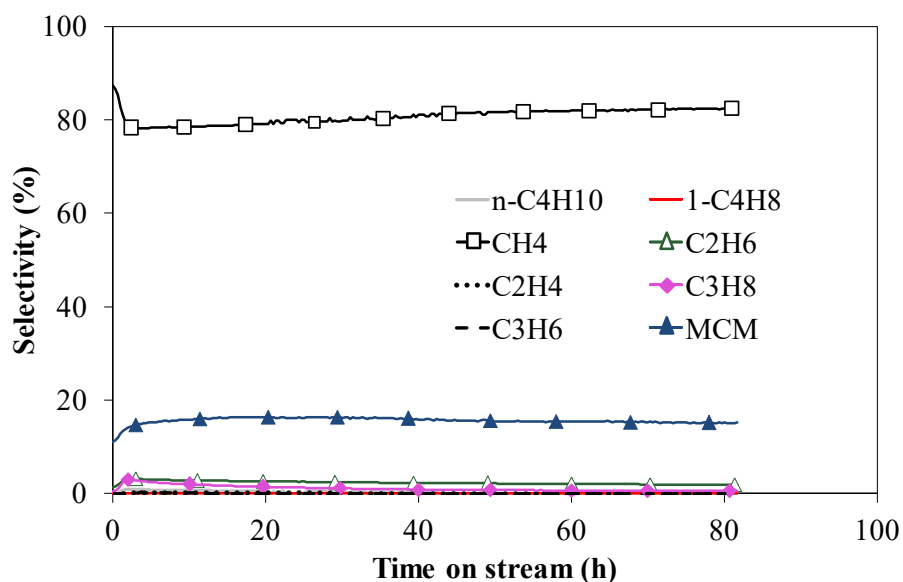


Figure 8. Selectivity to reaction products of the SZ Pt-Pd catalyst upon time on stream (space time = $0.8 \text{ kg}_{\text{cat}} \cdot \text{h} \cdot (\text{mol DCM})^{-1}$; $T = 250 \text{ }^{\circ}\text{C}$).

For the sake of comparison, Figure 9 shows the evolution of selectivity to reaction products upon time on stream for one of the catalysts that suffered rapid deactivation (WZ Pt-Pd). For the rest of the catalysts these results are provided as Supplementary information (Figures S6 to S8). Methane was always the main reaction product and in general no significant variations of selectivity were observed along the experiment. Deactivation seems to inhibit somewhat the deep hydrogenation of the olefinic byproducts as indicated by the slow decrease of the selectivity to alkanes other than CH_4 (ethane, propane and n-butane) and the increase of that to ethylene and propylene which can be appreciated in figure 9. The SZ Pt catalyst was the only one suffering a great deactivation among the SZ-supported catalysts tested. This can be explained by its higher interaction with the support as evidenced by TPR (Figure 1). In this catalyst the

metallic particles are more equally distributed between the outer surface and the internal porosity (Table 2) and a higher proportion of electrode deficient Pt was measured by XPS (Table 3).

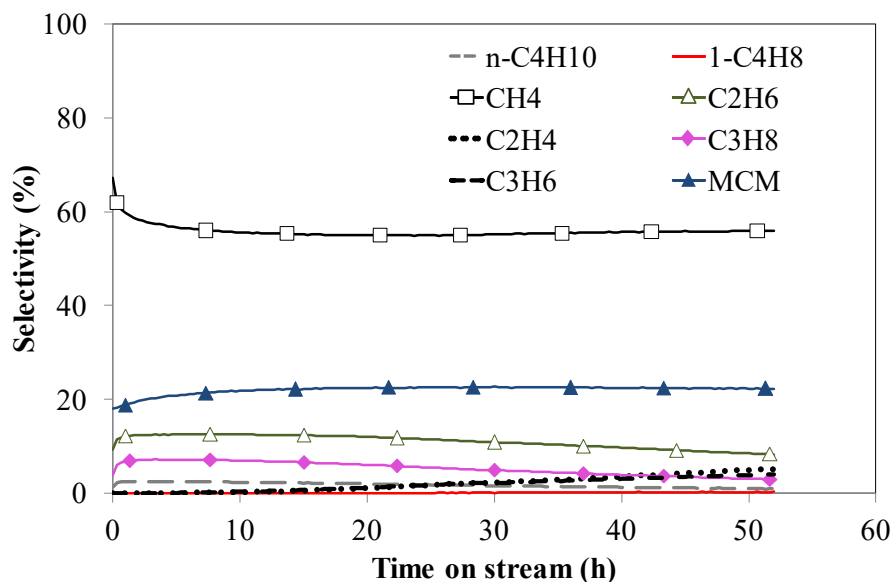


Figure 9. Selectivity to reaction products of the WZ Pt-Pd catalyst upon time on stream (space time = $0.8 \text{ kg}_{\text{cat}} \cdot \text{h} \cdot (\text{mol DCM})^{-1}$; $T = 250 \text{ }^{\circ}\text{C}$).

3.4. Characterization of the used catalysts

The XRD patterns (not represented) of the SZ and WZ catalysts after used in the long term experiments showed no significant changes with respect to those of the fresh reduced ones. This suggests that no significant modification of the size of the metallic particles takes place during the HDC process. Table 5 shows the bulk elemental analyses of the fresh and used catalysts. It is noteworthy the increase of carbon content of all the catalysts after use which is significantly more accused in those showing faster deactivation (see Figure 7). These results support the strong adsorption of organic species that would provoke blockage of the active sites as a cause of deactivation. The surface concentration (as determined by XPS) of Cl of the low-stability WZ catalysts used was between three and five times higher than in the fresh ones, thus supporting the

adsorption of chlorine-containing organic species on the used catalysts. Table 4 also shows a significant reduction of the sulfur content of the SZ catalysts after use. It is known that the catalysts based on sulfated zirconia can lose sulfur when submitted at a relatively high temperature in the presence of hydrogen [64,65]. This decrease of sulfur is due to the SO_4^- reduction to SO_2 , which in the presence of platinum is further reduced to H_2S . According to van Gestel et al [66] SO_4^- can be reduced at temperatures as low as 150 °C in the presence of platinum. Therefore, the presence of Pt would favor the loss of sulfur of the SZ-supported catalysts in agreement with the results reported in Table 4. The H_2S formed upon SO_4^- reduction would provoke poisoning of Pt thus explaining the poor stability of the SZ Pt catalyst in contrast to SZ Pd and SZ Pt-Pd. In fact, although the bulk S content of the SZ Pt catalyst used is very low (0.03%w in Table 4), the surface S concentration, as determined by XPS was 0.5%w.

Table 5. Elemental C and S content of the fresh (reduced) and used catalysts.

	%C	%S
<i>Fresh catalysts</i>		
SZ Pd		1.42
SZ Pt		1.40
SZ Pt-Pd		1.30
<i>Used catalysts</i>		
SZ Pd	0.18	0.90
SZ Pt	1.49	0.03
SZ Pt-Pd	0.76	0.43
WZ Pd	1.26	
WZ Pt	2.25	
WZ Pt-Pd	1.00	

Figure 10 represents the N_2 adsorption-desorption isotherms of SZ Pt-Pd and WZ Pt catalysts fresh and after used in the hydrodechlorination of DCM. We have represented the results of a catalyst with high stability (SZ Pt-Pd) and one of the catalysts with a fast deactivation rate (WZ Pt). In the case of the catalyst with a high stability, the decrease in the amount of N_2 adsorbed is almost negligible, indicating that no blocking of the

porous structure takes place during the hydrodechlorination reaction on this catalyst. Only a very slight reduction in the amount of N₂ adsorbed at low relative pressures is observed, which suggests a low significant reduction of the micropore volume. On the other hand, WZ Pt catalyst, shows a significant reduction of the volume of N₂ adsorbed at high relative pressure ($P/P_0 > 0.8$). This indicates that in the case of the catalysts that suffer deactivation, a significant decrease in the amount of mesopores takes place during the dehydrodechlorination reaction. This behavior is in agreement with the lower amount of carbon and/or organochlorides compounds deposited on the surface of the more stable catalysts (SZ Pd and SZ Pt-Pd), as shown by ultimate analyses and XPS, in contrast with the significant increase in the amount of carbon and chlorine observed for the catalysts that suffer deactivation, possibly by deposition of organochlorides compounds on the wider pores blocking the accesses to the reaction sites.

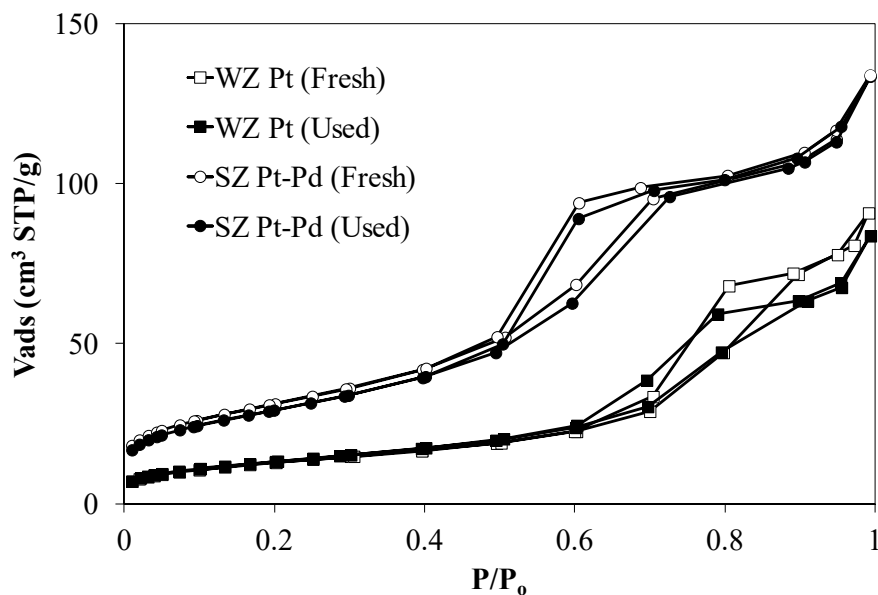


Figure 10. N₂ adsorption-desorption isotherms of SZ Pt-Pd and WZ Pt catalysts fresh and after used in the hydrodechlorination of DCM.

Conclusions

The Pd and Pt mono- and bimetallic catalysts prepared using zirconia promoted with sulfate (SZ) and tungsten oxide (WZ) as supports were fairly active in the hydrodechlorination reaction of DCM, though, in general the WZ catalysts yielded significantly higher DCM conversion values than the SZ ones. All the catalysts were very selective to non-chlorinated reaction products, the higher selectivities being obtained with the sulfated zirconia-supported Pd-Pt and Pd catalysts. The selectivity to monochloromethane decreased when increasing the reaction temperature except with the monometallic ~~palladium~~ platinum catalysts where that selectivity remained almost constant within the temperature range tested (150-250 °C). Methane was the main reaction product in all the cases. Ethane, propane, n-butane and 1-butene were also identified as byproducts. In addition, ethylene and propylene were detected in long-term experiments. The catalysts supported on tungstated zirconia showed a very poor stability regardless of the metal active phase. On the opposite, the palladium-containing catalysts supported on sulfated zirconia showed a high stability, in particular the bimetallic catalyst, demonstrated in long-term experiments (80 h on stream). The high stability of SZ Pt-Pd catalyst can be ascribed to the smaller size of metallic particles and a uniform distribution of the particles on the outer surface of the support, which hinder the poisoning of active centers by organochlorinated compounds. Deactivation of the other catalysts can be attributed to the deposition of chlorinated organic species blocking the active sites and, in the case of SZ platinum catalyst, also to poisoning by the H₂S resulting from SO₄⁼ reduction in the presence of hydrogen.

Acknowledgements

The authors are grateful to the Spanish “Ministerio de Ciencia e Innovación (MICINN)” for financial support (projects CTM2008-04751 and CTM2011-28352). J. Bedia acknowledges the Spanish MICINN for financing his research through the “Juan de la Cierva” post-doctoral program. M. Martín Martínez also wishes to thank the MICINN and the European Social Found for her research grant.

References

-
- [1] W.J. Hayes, E.R. Laws, *Handbook of Pesticide Toxicology*, Academic Press, San Diego, 1991.
- [2] E. Dobrzynska, M. Posniak, M. Szewczynska, B. Buszewski, *Crit. Rev. Anal. Chem.* 40 (2010) 41-57.
- [3] N.P. Cheremisinoff, *Industrial Solvents Handbook*, Marcel Dekker Inc., New York, 2003.
- [4] E. Lopez, S. Ordoñez, F.V. Diez, *Appl. Catal. B Environ.* 62 (2006) 57-65.
- [5] E. López, S. Ordoñez, H. Sastre, F.V. Diez, *J. Hazard. Mater.* 97 (2003) 281-294.
- [6] L. Prati, M. Rossi, *Appl. Catal. B Environ.* 23 (1999) 135-142.
- [7] A. Malinowski, D. Lomot, Z. Karpinski, *Appl. Catal. B – Environ.* 19 (1998) L79-L86.
- [8] T. Mori, T. Kikuchi, J. Kubo, Y. Morikawa, *Chem. Lett.* 30 (2001) 936-938.
- [9] B. Aristizabal, C.A. Gonzalez, I. Barrio, M. Montes, C.M. de Correa, *J. Mol. Catal. A Chem.* 222 (2004) 189-198.
- [10] C.A. Gonzalez, M. Bartoszek, A. Martin, C. Montes de Correa, *Ind. Eng. Chem. Res.* 48 (2009) 2826-2835.
- [11] M. Bonarowska, A. Malinowski, Z. Karpinski, *Appl. Catal. A: Gen.* 188 (1999) 145-154.
- [12] M. Martino, R. Rosal, H. Sastre, F.V. Díez, *Appl. Catal. B Environ.* 20 (1999) 301-307.
- [13] C.A.G. Sanchez, C.O.M. Patino, C. Montes de Correa, *Catal. Today* 133–135 (2008) 520-525.
- [14] P. Forni, L. Prati, M. Rossi, *Appl. Catal. B Environ.* 14 (1997) 49-53.
- [15] S. Ordoñez, F.V. Diez, H. Sastre, *Appl. Catal. B Environ.* 31 (2001) 113-122.
- [16] B. Heinrichs, F. Noville, J. Schoebrechts, J. Pirard, *J. Catal.* 220 (2003) 215-225.
- [17] D. Chakraborty, P.P. Kulkarni, V.I. Kovalchuk, J.L. d'Itri, *Catal. Today* 88 (2004) 169-181.
- [18] M. Legawiec-Jarzyna, A. Srebowata, W. Juszczak, Z. Karpinski, *J. Mol. Catal. A Chem.* 224 (2004) 171-177.
- [19] C. Amorim, G. Yuan, P.M. Patterson, M.A. Keane, *J. Catal.* 234 (2005) 268-281.
- [20] S. Ordóñez, E. Díaz, R.F. Bueres, E. Asedegbega-Nieto, H. Sastre, *J. Catal.* 272 (2010) 158-168.
- [21] S.Y. Kim, H.C. Choi, O.B. Yanga, K.H. Lee, J.S. Lee, Y.G. Kim, *J. Chem. Soc. Chem. Commun.* (1995) 2169-2170.
- [22] Z.M. de Pedro, L.M. Gomez-Sainero, E. Gonzalez-Serrano, J.J. Rodriguez, *Ind. Eng. Chem. Res.* 45 (2006) 7760-7766.
- [23] M.A. Álvarez-Montero, L.M. Gomez-Sainero, J. Juan-Juan, A. Linares-Solano, J.J. Rodriguez, *Chem. Eng. J.* 162 (2010) 599-608.
- [24] Z.M. de Pedro, J.A. Casas, L.M. Gomez-Sainero, J.J. Rodriguez, *Appl. Catal. B Environ.* 98 (2010) 79-85.
- [25] M.A. Álvarez-Montero, L.M. Gomez-Sainero, M. Martín-Martínez, F. Heras, J.J. Rodriguez, *Appl. Catal. B Environ.* 96 (2010) 148-156.
- [26] S. Omar, J. Palomar, L. M. Gómez-Sainero, M. A. Álvarez-Montero, M. Martín-Martínez, J. J. Rodríguez, *J. Phys. Chem. C* 115 (2011) 14180-14192.
- [27] M.A. Álvarez-Montero, L.M. Gómez-Sainero, A. Mayoral, I. Diaz, R.T. Baker, J.J. Rodríguez, *J. Catal.* 279 (2011) 389-396.

-
- [28] M.A. Álvarez-Montero. Hidrodecloración catalítica de clorometanos en fase gas mediante catalizadores metálicos soportados sobre carbones activos. Thesis, University Autónoma of Madrid, Spain, 2012.
- [29] M. Busto, J.M. Grau, C.R. Vera, *Appl. Catal. A Gen.* 387 (2010) 35-44.
- [30] M. Busto, C.R. Vera, J.M. Grau, *Fuel Process. Technol.* 92 (2011) 1675-1684.
- [31] S. Brunauer, P.H. Emmett, E. Teller, *J. Am. Chem. Soc.* 60 (1938) 309-319.
- [32] C.D. Wagner, L.E. Davis, M.V. Zeller, J.A. Taylor, R.H. Raymond, L.H. Gale, *Surf. Interface Anal.* 3 (1981) 211-225.
- [33] S.H. Ali, J.G. Goodwin, *J. Catal.* 176 (1998) 3-13.
- [34] N. Mahata, V. Vishwanathan, *Catal. Today* 49 (1999) 65-69.
- [35] R. Navarro, B. Pawelec, J.M. Trejo, R. Mariscal, J.L.G. Fierro, *J. Catal.* 189 (2000) 184-194.
- [36] V.L. Barrio, P.L. Arias, J.F. Cambra, M.B. Güemez, B. Pawelec, J.L.G. Fierro, *Appl. Catal. A* 242 (2003) 17-30.
- [37] A.M. Fuente, G. Pulgar, F. González, C. Pesquera, C. Blanco, *Appl. Catal. A* 208 (2001) 35-46.
- [38] A. Arcoya, X.L. Seoane, J. Soria, *J. Chem. Technol. Biotechnol.* 68 (1997) 171-176.
- [39] S.R. Vaudagna, R.A. Comelli, N.S. Figoli, *Appl. Catal. A* 164 (1997) 265-280.
- [40] J.F. Moulder, W.F. Stickle, P.E. Sobol, K.D. Bomben, in: J. Chastain, R.C. King, Jr. (Eds.), *Handbook of X-ray Photoelectron Spectroscopy*, Physical Electronics, Inc., Eden Prairie, MN, 1995.
- [41] O.B. Belskaya, I.G. Danilova, M.O. Kazakov, T.I. Gulyaeva, L.S. Kibis, A.I. Boronin, A.V. Lavrenov, V.A. Likholobov, *Appl. Catal. A Gen.* 387 (2010) 5-12.
- [42] Y. Shao, Z. Xu, H. Wan, H. Chen, F. Liu, L. Li, S. Zheng, *J. Hazard. Mat.* 179 (2010) 135-140.
- [43] A.M. Garrido Pedrosa, M.J.B. Souza, B.A. Marinkovic, D.M.A. Melo, A.S. Araujo, *Appl. Catal. A Gen.* 342 (2008) 56-62.
- [44] K. Persson, A. Ersson, S. Colussi, A. Trovarelli, S.G. Järås, *Appl. Catal. B Environ* 66 (2006) 175-185.
- [45] J.C. Yori, R.J. Gastaldo, V.M. Benítez, C.L. Pieck, C.R. Vera, J.M. Grau, *Catal. Today* 133-135 (2008) 339-343.
- [46] L. Calvo, A.F. Mohedano, J.A. Casas, M.A. Gilarranz, J.J. Rodríguez, *Carbon* 42 (2004) 1371-1375.
- [47] L. Calvo, M.A. Gilarranz, J.A. Casas, A.F. Mohedano, J.J. Rodríguez, *Ind. Eng. Chem. Res.* 44 (2005) 6661-6667.
- [48] J. Bedia, J.M. Rosas, J. Rodríguez-Mirasol, T. Cordero, *Appl. Catal. B: Environ.* 94 (2010) 8-18.
- [49] J.J. Carberry, in: J.R. Anderson, M. Boudart (Eds.), *Physicochemical Aspects of Mass Transfer and Heat Transfer in Heterogeneous Catalysis*, Springer-Verlag, Berlin, 1987.
- [50] O. Levenspiel, *Chemical Reactor Engineering: An Introduction to the Design of Chemical Reactors*, third ed., Wiley, New York, 1998.
- [51] A. Alvarez-Montero. Hidrodecloración catalítica de clorometanos en fase gas mediante catalizadores metálicos soportados sobre carbón activo. Ph.D. Thesis, University Autónoma of Madrid, Spain, 2011.
- [52] L.M. Gomez-Sainero, X.L. Seoane, J.L.G. Fierro, A. Arcoya, *J. Catal.* 209 (2002) 279-288.
- [53] P. Forni, L. Prati, M. Rossi, *Appl. Catal. B* 14 (1997) 49-53.

-
- [54] R. Gopinath, K. Narasimha Rao, P.S. Sai Prasad, S.S. Madhavendra, S. Narayanan, G. Vivekanandan, *J. Mol. Catal. A Chem.* 181 (2002) 215-220.
- [55] X. Zheng, Q. Xiao, Y. Zhang, X. Zhang, Y. Zhong, W. Zhu, *Catal. Today* 175 (2011) 615-618.
- [56] E. Díaz, S. Ordóñez, R.F. Bueres, E. Asedegbega-Nieto, H. Sastre, *Appl. Catal. B Environ.* 99 (2010) 181-190.
- [57] S. Ordóñez, E. Díaz, R.F. Bueres, E. Asedegbega-Nieto, H. Sastre, *J. Catal.* 272 (2010) 158-168.
- [58] T.F. Garetto, C.I. Vignatti, A. Borgna, A. Monzón, *Appl. Catal. B Environ.* 87 (2009) 211-219.
- [59] S. Ordóñez, H. Sastre, F.V. Díez, *Appl. Catal. B Environ.* 40 (2003) 119-130.
- [60] R. Gopinath, N. Lingaiah, B. Sreedhar, I. Suryanarayana, P.S. Sai Prasad, A. Obuchi, *Appl. Catal. B Environ.* 46 (2003) 587-594.
- [61] S. Ordóñez, H. Sastre, F.V. Díez, *Appl. Catal. B Environ.* 34 (2001) 213-226.
- [62] E.J. Creyghton, M.H.W. Burgers, J.C. Jansen, H. van Bekkum, *Appl. Catal. A Gen.* 128 (1995) 275-288.
- [63] T. Mori, T. Yasuoka, Y. Morikawa, *Catal. Today* 88 (2004) 111-120.
- [64] B.-Q. Xu, W.M.H. Sachtler, *J. Catal.* 167 (1997) 224-233.
- [65] J.M. Grau, J.C. Yori, C.R. Vera, F.C. Lovey, A.M. Condóc, J.M. Parera, *Appl. Catal. A Gen.* 265 (2004) 141-152.
- [66] J. van Gestel, Vu T. Nghiem, D. Guillaume, J. P. Gilson, J. C. Duchet, *J. Catal.* 212 (2002) 173-181.